Molecular Crystals and Liquid Crystals
Publication details, including instructions for authors and subscription information:
http://www.tandfonline.com/loi/gmcl20

Achromatic Liquid Crystal Phase Plate for Short Laser Pulses

Ru-Pin Pan [a], Cheng-Wei Lai [a], Chia-Jen Lin [a], Cho-Fan Hsieh [a] & Ci-Ling Pan [b]

[a] Department of Electrophysics, National Chiao Tung University, Hsinchu, Taiwan, Republic of China

[b] Department of Physics and Inst. of Photonic Technologies, National Tsing Hua University, Hsinchu, Taiwan, Republic of China
Published online: 19 Aug 2010.

To cite this article: Ru-Pin Pan, Cheng-Wei Lai, Chia-Jen Lin, Cho-Fan Hsieh & Ci-Ling Pan (2010) Achromatic Liquid Crystal Phase Plate for Short Laser Pulses, Molecular Crystals and Liquid Crystals, 527:1, 65/[221]-71/[227], DOI: 10.1080/15421406.2010.486632

To link to this article: http://dx.doi.org/10.1080/15421406.2010.486632

Mol. Cryst. Liq. Cryst., Vol. 527: pp. 65/[221]–71/[227], 2010

ISSN: 1542-1406 print/1563-5287 online
DOI: 10.1080/15421406.2010.486632

Achromatic Liquid Crystal Phase Plate for Short Laser Pulses

RU-PIN PAN,[1] CHENG-WEI LAI,[1] CHIA-JEN LIN,[1] CHO-FAN HSIEH,[1] AND CI-LING PAN[2]

[1]Department of Electrophysics, National Chiao Tung University, Hsinchu, Taiwan, Republic of China
[2]Department of Physics and Inst. of Photonic Technologies, National Tsing Hua University, Hsinchu, Taiwan, Republic of China

This work demonstrates the feasibility of reducing pulse broadening by using liquid crystal achromatic half and quarter wave plates for ultrafast pulsed lasers. Each wave plate is made of two and three liquid crystal cells stacked together. Total phase retardation and its broadening reducing of the achromatic half wave plate have been measured. The experimental results are in good agreement with theoretical calculation.

Keywords Achromatic; liquid crystal; pulse width; ultrafast pulsed lasers; wave plate

1. Motivation

Liquid crystal has been widely used for phase retarders among which the quarter wave plates and half wave plates are the most common application [1,2]. Quarter and half wave plates can change a linearly polarized light into a circularly light and the polarization direction of a linearly polarized light, respectively. The phase retardation of a wave plate is strongly dependent on the wavelength of incident light and then the phase dispersion can cause pulse width broadening on the laser pulses. Considering a very short light pulse, its spectrum bandwidth ($\Delta\lambda$) is inversely proportional to its pulse width (Δt). In other words, short pulses have large wavelength bandwidth. Figure 1. shows the specturm of our Ti:Sppphire ultrafast laser with central wavelength around 800 nm. The bandwidth is 40 nm and the pulse width is less than 100 fs.

In order to maintain the short pulse width, the waveplates must be achromatic. Achromatic wave plates had been suggested by Kohns et al by using liquid crystal mixture which has an birefringence (Δn) varies proportional to wavelength [3]. On the other hand, an equivalent achromatic wave plate can be obtained by combining

Address correspondence to Ru-Pin Pan, Department of Electrophysics, National Chiao Tung University, Hsinchu, Taiwan 30010, Republic of China. Tel.: +886-3-5731989; Fax: +886-3-5725230; E-mail: rpchao@mail.nctu.edu.tw

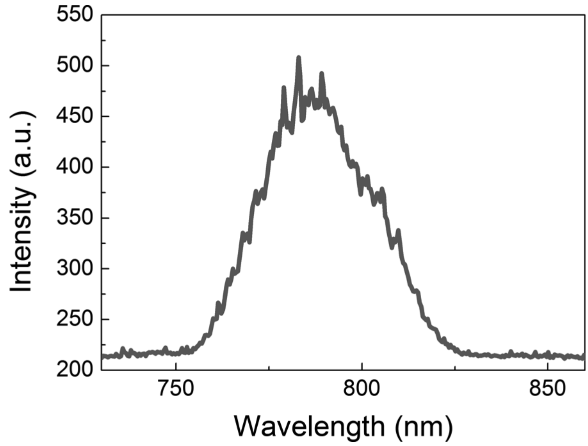

Figure 1. The spectrum of Ti:Sapphire ultrafast laser.

several wave plates. Similar idea had been used in reflection liquid crystal displays [4,5], and terahertz wave plates [6]. In this work, we use several electric tunable liquid crystal cells to create achromatic wave plates. The effect on reducing the pulse width broadening is studied. The phase retardation of each cell can be easily modulated by controlling the applied voltage.

2. Theory and Design

We use Stokes representation and Poincarè sphere [7] to predict the variation of polarization state of laser pulses after passing through our devices. A conventional quarter wave plate which is made of dispersionless material and designed for 550 nm has a phase retardation of 0.5π only for this wavelength. For wavelength 450 nm and 650 nm the phase retardations are 0.61π and 0.42π, respectively. When the slow axis of the quarter wave plate is 45° to x-axis, the horizontal polarization of incident light will be changed into circular polarization only for the wavelength of 550 nm. The polarization state of output laser pulses will not be circular at 450 nm and 650 nm [see Fig. 2].

In our design for achromatic quarter wave plate, a half wave plate and a quarter wave plate are stacked with an angle of 60° between their slow axes. The achromatic half wave plate is formed with three half wave plates. The outer wave plates are aligned with their slow axes parallel while the middle wave plate has its slow axis at an angle of 60° with respect to the outer ones. As shown in Figure 3, the polarization states of output laser pulses are very close to circular polarized waves and vertical polarized waves after passing through an achromatic quarter and half wave plate even for 450 nm and 650 nm, respectively.

We also use Jones matrix method [6] to calculate the wavelength dependency of the devices. Each plate in our designed can be described by a corresponding Jones matrix J_i,

$$J_i(\delta_i, \theta_i) = \begin{bmatrix} \cos\delta_i/2 - i\cos 2\theta_i \sin\delta_i/2 & -i\sin 2\theta_i \sin\delta_i/2 \\ -i\sin 2\theta_i \sin\delta_i/2 & \cos\delta_i/2 + i\cos 2\theta_i \sin\delta_i/2 \end{bmatrix}, \quad (1)$$

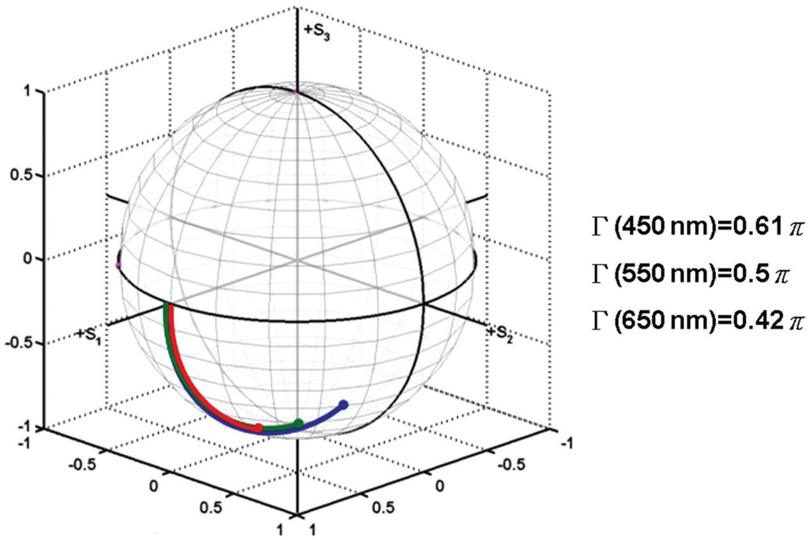

Figure 2. Poincaré sphere representation of polarzation state evolution through a quarter wave plate.

where δ_i is the phase retardation $\delta_i = 2\pi(n_e\text{-}n_o)d_i/\lambda$ and θ_i is the angle between the slow axis and x-axis. Since Jones matrix is a unitary matrix, the combined Jones matrix has a form of

$$J = \prod_i J_i = \begin{bmatrix} A & B \\ -B^* & A^* \end{bmatrix} \qquad (2)$$

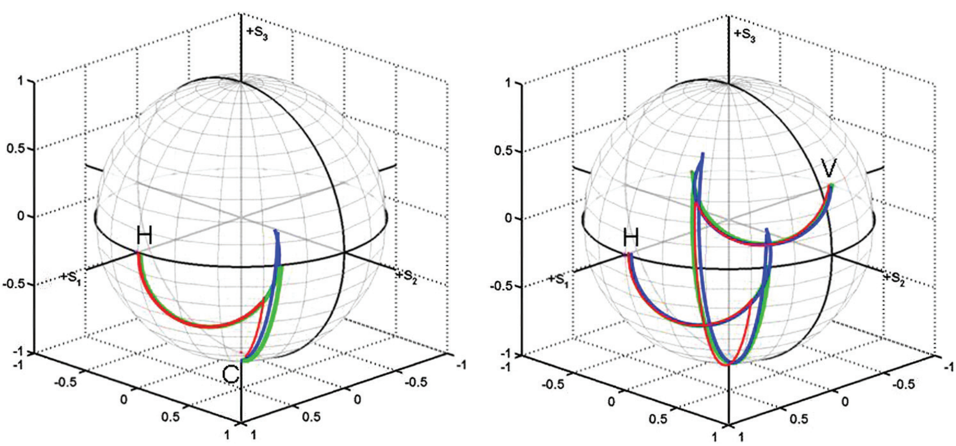

Figure 3. (a) The horizontal polarization (H) changes to circular polarization (C) after passing through an achromatic quarter wave plate and the slow axes of the quarter and half wave plates are 15° and 75° to x-axis, (b) the horizontal polarization (H) changes to vertical polarization (V) after passing through an achromatic half wave plate and the slow axes of each half plates are 15°, 75° and 15° to x-axis.

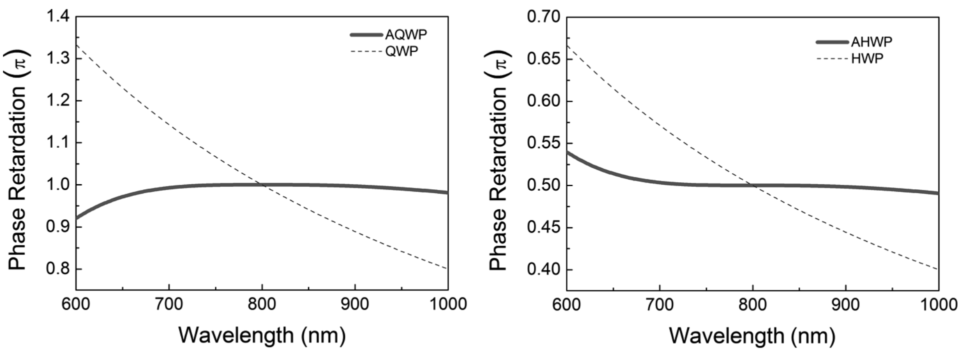

(a) (b)

Figure 4. Relationship between phase retardation and wavelength: (a) solid line: AQWP; dashed line: QWP, (b) solid line: AHWP; dashed line: HWP.

and the total phase retardation δ is obtained by

$$\tan^2\frac{\delta}{2} = \frac{|\mathrm{Im}\,A|^2+|\mathrm{Im}\,B|^2}{|\mathrm{Re}\,A|^2+|\mathrm{Re}\,B|^2}. \tag{3}$$

By using Jones matrix calculation, we can find out the relationship between phase retardation and wavelength of our design. Figure 4 shows that there is a wavelength region with the phase retardation is insensitive to wavelength (solid line). The biggest error in ± 200 nm are 7.96% and 8.00% at 600 nm for an achromatic quarter wave plate (AQWP) and an achromatic half wave plate (AHWP), respectively. The dashed lines are non-achromatic QWP and HWP.

Our wave plates are rubbed antiparallel cells filled with nematic liquid crystal (E7). The direction of slow axis is the same as rubbing direction and the phase retardation are controlled by applied voltage.

3. Phase Retardation Measurement

The phase retardation of our devices was measured with a setup as shown in Figure 5 [8]. The light source is a Ti:Sapphire laser working at continuous wave mode.

The linearly polarized light passing through a modulator cell M (a nematic liquid crystal cell) is incident on a beam splitter BS and is divided into two parts: the reference beam and the test beam. The reference beam passes through an analyzer A_r, then is detected by photodetector D_r. The test beam passes through a tested achromatic wave plate (AWP) and an analyzer A_t and is detected by another photodector D_t. The polarization axis of polarizer is along the x-direction, while both analyzers are perpendicular to the polarizer. The z axis is in the propagation direction. The slow axis of M and the equivalent slow axis of AWP are both at 45° to the x axis. The normalized intensity of the reference beam and the test beam obtained by applying Jones matrix method are as following:

$$I_r = Sin^2\frac{\Gamma_M}{2}, \tag{4}$$

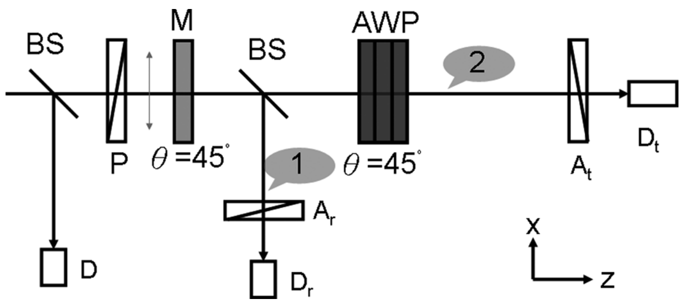

Figure 5. Schematic diagram for measuring the phase retardation of AWP: 1, reference beam; 2, test beam; M, modulator cell; BS, beam splitter; AWP, achromatic wave plate; P, polarizer; A, analyzer; D, photodetector.

$$\text{and} \quad I_t = Sin^2 \frac{\Gamma_M + \delta}{2}, \tag{5}$$

where Γ_M is the phase retardation introduced by the modulator cell and δ is the phase retardation to be measured. We varied the applied voltage on M from 0.1 V to 10 V a range in which Γ_M had a total change slightly over 2π as shown by the red circles in Figure 6. Then we also observed a intensity detected by A_t varies accordingly as shown by the black square dots. The phase retardation δ was then deduced following Eqs. (4) and (5).

The measured phase retardation of the AHWP are shown in Figure 7 with the theoretical calculated results. The solid line and dashed line repersent the theoretical results for an AHWP and a 0th order non-achromatic HWP, respectively and the square dots represent the experimental data. It is clearly shown that the phase retardations for the light with wavelength between 740–850 nm are remained at π after passing through the AHWP, which agrees with the theoretical prediction.

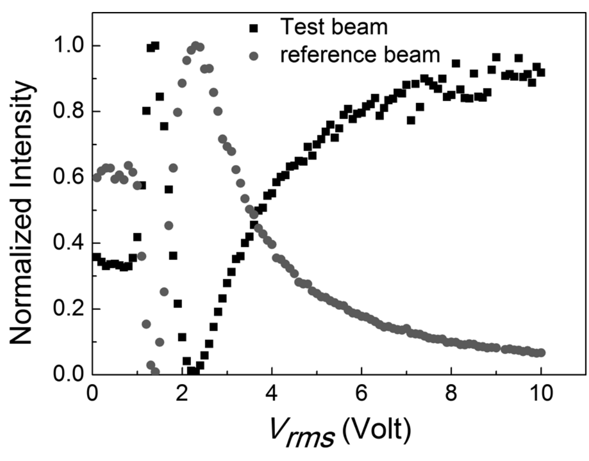

Figure 6. Normalized intensity versus the applied voltage on M at 800 nm: square dots, the test beam; dots, the reference beam.

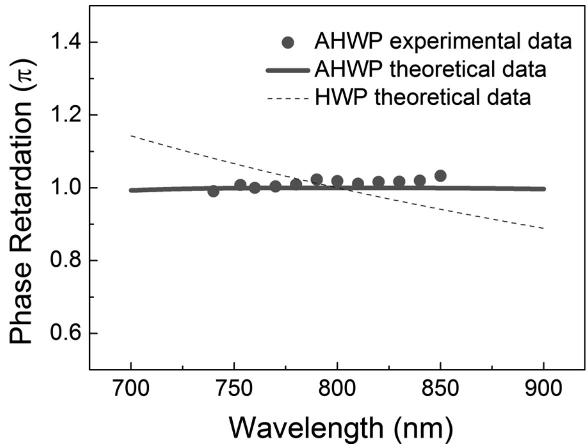

Figure 7. Phase retardation versus wavelength of the half wave plate. Solid line: theoretical data of the AHWP; Dashed line: theoretical data of the 0th order HWP; Square dots: experimental data of the AHWP.

4. Application to Ultrafast Laser Pulses

We used interferometric autocorrelation [9] to measure the full width half maximum (FWHM) of the pulses and their broadening caused by phase retarders. The FWHM of incident pulse is 61.48 fs. The FWHMs are 63.34 fs and 74.52 fs after passing through the achromatic quarter and half wave plate while the FWHMs are 67.03 fs and 83.83 fs after passing through the 0th order non-achromatic wave plates, respectively. The device we designed can reduce the effect of pulse broadening due to the wavelength dispersion in regular wave plates. Next, we consider the pulse broadening caused by material dispersion of glass substrates and liquid crystal. The relation of pulses width between the incident beam and output beam is given by [10],

$$\Delta t' = \Delta t\sqrt{1 + \left(\frac{4\ln 2 \times K''}{\Delta t^2}\right)^2}, \tag{6}$$

Here, Δt and $\Delta t'$ are the FWHMs of the incident and the output pulses, respectively and K'' is the group dispersion delay (GDD) of the glass substrates and liquid crystal. We have measured the pulse width of the incident pulse and the pulse after passing through a glass substrate and 24 μm thick liquid crystal cell. By using Eq. (6), we determine that the GDD of one glass substrate is 97.48 fs^2 and the GDD of a 3 μm layer of liquid crystal is 1.28 fs^2. For a liquid crystal sample including two glass substrates and a 3 μm layer of liquid crystal, the GDD of liquid crystal is thus 0.66% that of the substrates. The pulse broadening is entirely contributed caused by the material dispersion of glass substrates.

5. Conclusion and Future Work

We have succeessfully demonstrated a new type of achromatic half wave plates and quarter wave plates. Comparing to comercial AWP, our achromatic region can be varied by changing applied voltage to each plate. The substrate group velocity dispersion is now the main reason for pulse broadening. Improved performance is expected by empolying thinner substrates or a sandwich-type device.

References

[1] Wu, H.-Y., Hsieh, C.-F., Tang, T.-T., Pan, R.-P., & Pan, C.-L. (2006). Electrically tunable room-temperature 2-pi liquid crystal terahertz phase shifter. *IEEE Photonics Technology Letters*, *18*, 1488–1490.

[2] Chen, C.-Y., Hsieh, C.-F., Lin, Y.-F., Pan, R.-P., & Pan, C.-L. (2004). Magnetically tunable room-temperature 2π liquid crystal terahertz phase shifter. *Optics Express*, *12*, 2625–2630.

[3] Kohns, P., Schirmer, J., Muravski, A. A., Yakovenko, S. Y., & Dabrowski, R. (1996). Bireferingence measurements of liquid crystals and an application: an achromatic waveplate. *Liquid Crystals*, *21*, 841–846.

[4] Yu, C.-J., Kim, J.-H., & Lee, S.-D. (2002). Qusasi-achromatic and wide viewing properties of a reflective liquid crystal display in in-plane optical geometry. *Jpn. J. Appl. Phys.*, *41*, 5298–5301.

[5] Ge, Z., Wu, T.-X., Zhu, X., & Wu, S.-T. (2005). Reflective liquid-crystal displays with asymmetric incident and exis angle. *J. Opt. Soc. Am.*, *22*, 966–977.

[6] Masson, J. B., & Gallot, G. (2006). Terahertz achromatic quarter-wave plate. *Optics Letters*, *31*, 265–267.

[7] Yeh, P., & Gu, C. (1999). *Optics of Liquid Crystal Display*, Chapter 2, Wiley Interscience Publication: New York, 36.

[8] Shyu, L.-H., Chen, C.-L., & Su, D.-C. (1993). Method for measuring the phase retardation of a wave plate. *Appl. Opt.*, *32*, 4228–4230.

[9] Chen, C.-W., Huang, J.-Y., & Pan, C.-L. (2006). Pulse retrieval from interferometric autocorrelation measurement by use of the population-split genetic algorithm. *Optics Express*, *14*, 10930–10938.

[10] Hirlimann, C. (2005). Pulsed optics. Chapter 2, In: *Femtosecond Laser Pulses: Principles and Experiments*, 2nd. Ed., Rullière, G. (Ed.), Springer: New York, 32.